Article

Cell Reports

IL-38 Ameliorates Skin Inflammation and Limits IL-17 Production from γδ T Cells

Graphical Abstract

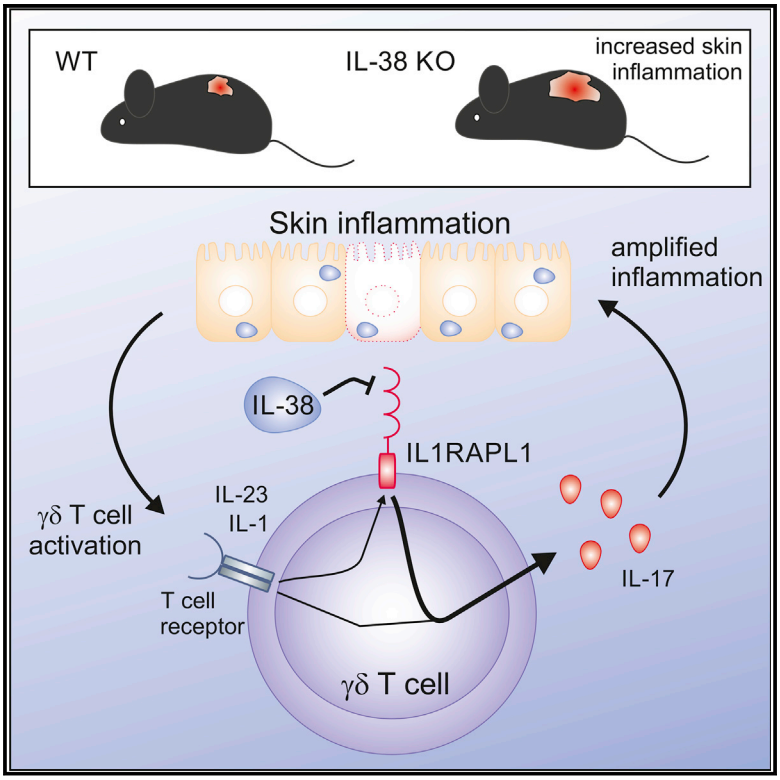

Authors

Yingying Han, Javier Mora, Arnaud Huard, ..., Andreas Ernst, Bernhard Brüne, Andreas Weigert

Correspondence

weigert@biochem.uni-frankfurt.de

In Brief

Han et al. report that genetic depletion of IL-38 in mice delays the resolution of imiquimod-induced psoriasis by increasing the production of the inflammatory cytokine IL-17A by skin-infiltrating T cells. Depleting these T cells or the receptor that is targeted by IL-38 reduces psoriatic skin inflammation.

Highlights

- IL-38-deficient mice display delayed resolution of imiquimod-induced psoriasis
- IL-38 suppresses IL-17A production by γδ T cells
- Inhibition of IL-17A production by γδ T cells requires IL1RAPL1
- IL1RAPL1-deficient mice show decreased γδ T cell activation during psoriasis

Han et al., 2019, Cell Reports *27*, 835–846
April 16, 2019
https://doi.org/10.1016/j.celrep.2019.03.082

CellPress

Cell Reports
Article

IL-38 Ameliorates Skin Inflammation and Limits IL-17 Production from γδ T Cells

Yingying Han,[1,2,3,12] Javier Mora,[1,4,12] Arnaud Huard,[1] Priscila da Silva,[1] Svenja Wiechmann,[5,6] Mateusz Putyrski,[6] Christian Schuster,[1] Eiman Elwakeel,[1] Guangping Lang,[7] Anica Scholz,[1] Tatjana Scholz,[8] Tobias Schmid,[1] Natasja de Bruin,[6] Pierre Billuart,[9] Carlo Sala,[10,11] Harald Burkhardt,[6,8] Michael J. Parnham,[6] Andreas Ernst,[5,6] Bernhard Brüne,[1,6] and Andreas Weigert[1,13,*]

[1]Institute of Biochemistry I, Faculty of Medicine, Goethe-University Frankfurt, 60590 Frankfurt, Germany
[2]Special Key Laboratory of Oral Diseases Research, Higher Education Institutions of Guizhou Province, Zunyi Medical University, 563006 Zunyi, Guizhou, China
[3]School of Stomatology, Zunyi Medical University, 563006 Zunyi, Guizhou, China
[4]Faculty of Microbiology, University of Costa Rica, 2060 San José, Costa Rica
[5]Institute of Clinical Pharmacology, Pharmazentrum Frankfurt/ZAFES, Faculty of Medicine, Goethe-University Frankfurt, 60590 Frankfurt am Main, Germany
[6]Branch for Translational Medicine and Pharmacology TMP, Fraunhofer Institute for Molecular Biology and Applied Ecology IME, 60590 Frankfurt, Germany
[7]Institute of Molecular Cell Biology, Center for Molecular Biomedicine (CMB), Jena University Hospital, 07745 Jena, Germany
[8]Division of Rheumatology, University Hospital Frankfurt, Goethe University, Frankfurt am Main, Germany
[9]Institut Cochin, Institut National de la Santé et de la Recherche Médicale U1016, Centre National de la Recherche Scientifique UMR8104, Université Paris Descartes, Paris 75014, France
[10]National Research Council Neuroscience Institute, 20129 Milan, Italy
[11]Department of Medical Biotechnology and Translational Medicine, Università degli Studi di Milano, 20129 Milan, Italy
[12]These authors contributed equally
[13]Lead Contact
*Correspondence: weigert@biochem.uni-frankfurt.de
https://doi.org/10.1016/j.celrep.2019.03.082

SUMMARY

Interleukin-38 (IL-38) is a cytokine of the IL-1 family with a role in chronic inflammation. However, its main cellular targets and receptors remain obscure. IL-38 is highly expressed in the skin and downregulated in psoriasis patients. We report an investigation in cellular targets of IL-38 during the progression of imiquimod-induced psoriasis. In this model, IL-38 knockout (IL-38 KO) mice show delayed disease resolution with exacerbated IL-17-mediated inflammation, which is reversed by the administration of mature IL-38 or γδ T cell-receptor-blocking antibodies. Mechanistically, X-linked IL-1 receptor accessory protein-like 1 (IL1RAPL1) is upregulated upon γδ T cell activation to feedforward-amplify IL-17 production and is required for IL-38 to suppress γδ T cell IL-17 production. Accordingly, psoriatic IL1RAPL1 KO mice show reduced inflammation and IL-17 production by γδ T cells. Our findings indicate a role for IL-38 in the regulation of γδ T cell activation through IL1RAPL1, with consequences for auto-inflammatory disease.

INTRODUCTION

Interleukin-1 (IL-1) family cytokines are crucial regulators of inflammation. IL-1 family receptor agonists usually promote, while receptor antagonists limit, inflammatory reactions. IL-38 is the most recently described and least understood cytokine of the IL-1 family (van de Veerdonk et al., 2018). IL-38 shows sequence similarity with the IL-1 family receptor antagonists IL-1Ra and IL-36Ra (Lin et al., 2001), indicating anti-inflammatory properties. IL-38 SNPs are associated with susceptibility to inflammatory diseases with a TH1 or TH17 etiology; most prominently, inflammatory arthritides (Guo et al., 2010; Jung et al., 2010; Rahman et al., 2006; Sims et al., 2008). Accordingly, overexpression of the IL-38 precursor reduced the severity of collagen-induced arthritis in mice, concomitant with reduced expression of disease-promoting cytokines, including IL-6 and tumor necrosis factor α (TNF-α) (Boutet et al., 2017). In this setup, macrophages were proposed as targets of IL-38, but the receptor antagonized by IL-38 was unclear. Mature IL-38 released from apoptotic cells limits IL-6 release from human macrophages and subsequent production of IL-17 by co-cultured human T cells *in vitro* by acting on IL-1 receptor accessory protein-like 1 (IL1RAPL1), an orphan IL-1 family receptor (Mora et al., 2016). Moreover, the IL-38 precursor antagonized the IL-36 receptor over a narrow concentration range, thereby attenuating *C. albicans*-induced TH17 cytokine production by human peripheral blood mononuclear cells (PBMCs) (van de Veerdonk et al., 2012). These data suggest that IL-38 has the capacity to limit chronic IL-17-dependent inflammation, although a number of questions remain. Cellular targets of IL-38 and the receptor(s) transducing the anti-inflammatory potential of IL-38 *in vivo* are obscure, since, in addition to IL-36R and IL-1RAPL1, IL-38 also binds with low affinity to IL-1R1 (Mora et al., 2016). Moreover, the role of endogenous IL-38

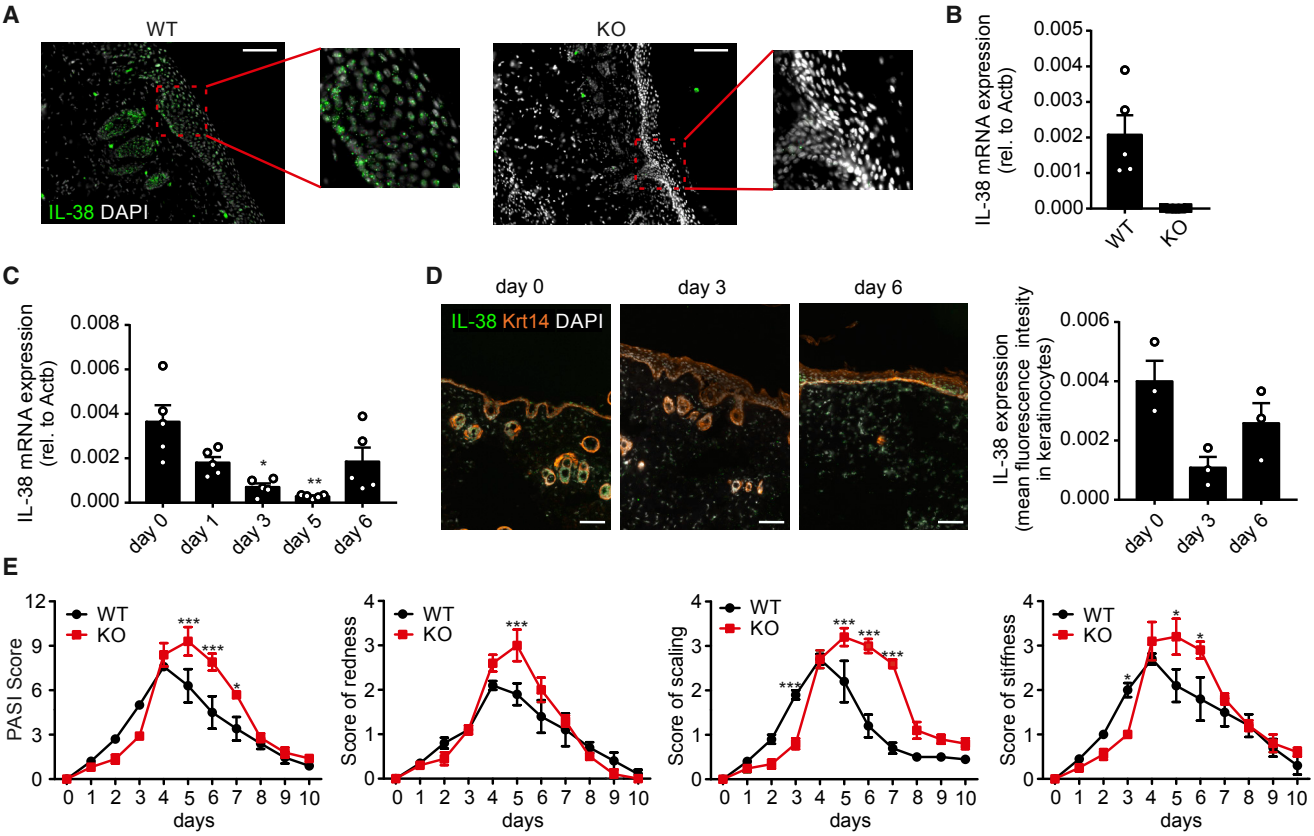

Figure 1. IL-38 KO Mice Develop Prolonged IMQ-Induced Skin Inflammation

Wild-type (WT) and IL-38 knockout (KO) mice were treated daily with 62.5 mg IMQ-containing cream on their back skin for 6 days and monitored for another 4 days.

(A) *In situ* hybridization by RNAScope indicates the expression of IL-38 in psoriatic skin at day 6. Nuclei were counterstained with DAPI. Scale bars represent 100 μm. Representative data are from three independent experiments.

(B) mRNA expression of IL-38 is indicated in WT and IL-38 KO mice at day 0. Data are means ± SEM of five individual animals each.

(C) IL-38 mRNA expression in psoriatic WT skin was quantified at times indicated. Data are means ± SEM of five individual animals each.

(D) *In situ* hybridization by RNAScope indicates the expression of IL-38 in psoriatic skin at times indicated. Nuclei were counterstained with DAPI. Scale bars represent 100 μm. The graph shows the quantification of mean IL-38 expression in keratinocytes. Data are means ± SEM of three individual animals each.

(E) Cumulative Psoriasis Area Severity Index (PASI) scores were calculated based on the individual scores for redness, scaling, and stiffness daily until 10 days after initial IMQ application. Data are means ± SEM of five individual animals each from three separate experiments.

All data are biological replicates. *$p < 0.05$; **$p < 0.01$; ***$p < 0.001$; p values were calculated using Kruskal-Wallis test with Dunn's correction (C and D) or two-way ANOVA with Bonferroni's correction (E).

during inflammation is unclear. So far, studies have focused on changes in IL-38 expression levels under inflammatory conditions (Boutet et al., 2016; Rudloff et al., 2015) or substituted IL-38 to ameliorate inflammation (Boutet et al., 2017; Chu et al., 2017).

In the present study, we set out to investigate whether endogenous IL-38 might restrict IL-17-dependent inflammation in the imiquimod (IMQ)-induced model of psoriasis. Psoriasiform inflammation in this model and human psoriasis depends on the IL-17A/IL-23 axis (van der Fits et al., 2009). IL-1 family cytokines, particularly members of the IL-36 subfamily to which IL-38 belongs, have been linked to psoriasis (Blumberg et al., 2010). Moreover, previous studies indicated reduced expression of IL-38 in psoriatic skin (Boutet et al., 2016). Therefore, we investigated the molecular and cellular targets of IL-38 during psoriasiform skin inflammation.

RESULTS

IL-38 Is an Endogenous Suppressor of Psoriasiform Skin Inflammation

By analyzing IL-38 transcripts using *in situ* hybridization, we observed predominantly epidermal expression of IL-38 in mouse skin (Figure 1A). As expected, IL-38 was absent in the skin of IL-38-deficient (IL-38 KO) mice (Figures 1A and 1B). In wild-type (WT) mice subjected to IMQ-induced psoriasis, IL-38 expression was continuously reduced until day 5, while expression increased again on day 6, when IMQ-induced psoriasis resolves (Figures 1C and 1D). The inverse pattern of IL-38 expression and skin inflammation, which was also apparent in a publicly available dataset of human psoriasis patients (Li et al., 2014a) (Figure S1), suggested an impact of IL-38 in IMQ-induced psoriasis. Indeed, clinical PASI scores suggested a

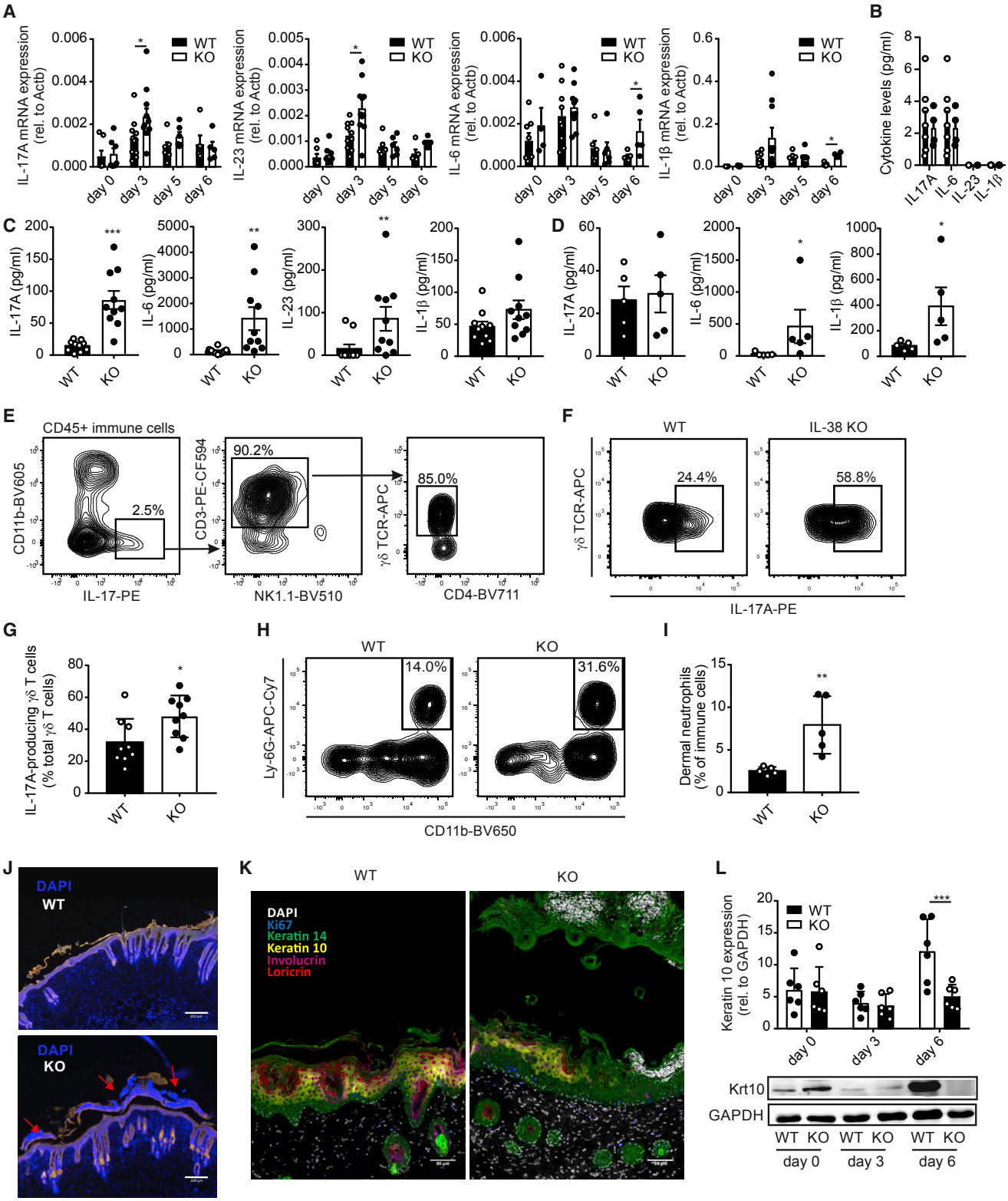

(legend on next page)

delayed resolution of skin inflammation in IL-38 KO mice, as indicated by increased inflammation and skin stiffness, as well as prolonged scaling from day 5 onward (Figure 1E).

IL-38 Suppresses IL-17 Production by Dermal γδ T Cells

Given the putative impact of IL-38 on IL-17 production, we next analyzed expression of cytokines involved in IL-17 generation, including IL-1, IL-6, and IL-23 (Sutton et al., 2009), as well as IL-17A itself. Time kinetics analysis of mRNA expression in IMQ-treated skin revealed a biphasic increase in inflammatory cytokine production in IL-38 KO skin, compared to WT skin, at days 3 and 6 (Figure 2A). Protein levels at the baseline (day 0) were unchanged (Figure 2B), whereas levels of IL-17A, IL-23, and IL-6 were elevated on day 3 in IL-38 KO skin. On day 6, only an increase in IL-6 and IL-1β was observed (Figures 2C and 2D). IL-17A is a major driver of IMQ-triggered skin inflammation. Flow-cytometric analysis of single-cell suspensions from whole skin of IMQ-treated WT and IL-38 KO mice revealed that, consistent with a previous study (Cai et al., 2011), dermal γδ T cell receptor $(TCR)^{low}$ γδ T cells were the major cellular source of IL-17A at day 3 (Figure 2E). Importantly, the percentage of dermal γδ TCR^{low} IL-17A-producing γδ T cells was significantly higher in IL-38 KO mice compared to WT mice (Figures 2F and 2G; gating strategy in Figure S2A). Apart from γδ T cells, natural killer T cells (NKT cells), natural killer cells (NK cells), and TH17 cells showed detectable IL-17A expression, but their IL-17 production was not increased in IL-38 KO skin (Figure S2B). IL-17A is a granulokine, and IL-17A release from γδ T cells was shown to increase neutrophil infiltrates during infection (Martin et al., 2009). Consequently, and in good correlation with PASI scores for increased redness, neutrophil infiltrates were significantly increased in the dermis of IMQ-treated IL-38 KO animals at day 5 (Figures 2H and 2I; gating strategy in Figure S2C), followed at day 6 by enhanced microabscess formation (dying neutrophils) in the epidermis (Figure 2J). The abundance of other skin immune cell subsets was not altered (Figure S3).

IL-38 Deficiency Delays Keratinocyte Regeneration

Inflammatory conditions trigger human keratinocyte dedifferentiation (Rabeony et al., 2014). Psoriasis is characterized by disturbed keratinocyte differentiation, and undifferentiated human keratinocytes show decreased IL-38 expression (Li et al., 2014b) similar to reduced IL-38 levels in psoriatic human and murine skin. Analysis of mRNA expression of the keratinocyte differentiation markers involucrin (Ivl) and loricrin (Lor), markers of the stratum granolusum and the stratum corneum, and keratin 10 (Krt10), a marker of the stratum spinosum, revealed disturbed keratinocyte differentiation in psoriatic IL-38 KO skin (Figure S4A). The expression of Lor and Krt10 was decreased when comparing day 0 to day 3, which was more prominent in IL-38 KO mice, indicating that IMQ-induced keratinocyte dedifferentiation occurred in IL-38 KO mice to a greater extent than in WT mice. The expression of Ivl, Lor, and Krt10 increased again on day 6 in WT mice, which was less prominent in IL-38 KO mice, suggesting a delay in skin regeneration. When looking at skin differentiation markers using multiplex histology on day 6, we found that WT mouse skin architecture returned to its characteristic layered appearance, although being still considerably thicker. In contrast, markers of keratinocyte differentiation were expressed at low levels in skin of IL-38 KO mice, accompanied by microabscesses and pronounced scaling (Figure 2K; Figure S4B). Quantitatively, Krt10 protein expression decreased from day 0 to day 3 and increased again on day 6 in WT but not in IL-38 KO skin (Figure 2L). Thus, IL-38 promotes keratinocyte differentiation.

Mature IL-38 Ameliorates Skin Inflammation in IL-38 KO Mice

We questioned whether the effects of IL-38 depletion in psoriatic IL-38 KO mice were truly IL-38 mediated and not due to compensatory pathways activated in IL-38 KO animals. Therefore, we performed rescue studies using in-house-generated human recombinant IL-38 in IL-38 KO mice. We previously described the release of a putatively mature, N-terminally processed form of IL-38 from apoptotic cells, which lacked the first six amino acids (IL-38 aa 7–152) (Mora et al., 2016). IL-36 subfamily cytokines are considerably more active when a few amino acids are removed from their N terminus (Towne et al., 2011). To identify the most potent IL-38 variant, we generated full-length IL-38 and various N-terminally truncated variants, including mature

Figure 2. Enhanced Inflammation and Delayed Skin Regeneration in Psoriatic IL-38 KO Mice

(A–K) Wild-type (WT) and IL-38 knockout (KO) mice were treated daily with 62.5 mg IMQ on the back skin for up to 6 days (see also Figures S2–S4).

(A) IL-17A, IL-23, IL-6, and IL-1β mRNA expression was quantified using qPCR at times indicated. Data are means ± SEM at seven (day 0), 10 (day 3), six (day 5), and five (day 6) individual animals each.

(B–D) Cytokine levels in skin at day 0 (B), day 3 (C), and day 6 (D) were determined using cytometric bead array. Data are means ± SEM of ≥4 (B), 10 (C), or 5 (D) individual animals each.

(E) Gating strategy to IL-17A-producing cell subsets in psoriatic mouse skin at day 3. IL-17-producing cells (which were CD11b−) in the total CD45+ fraction were identified by intracellular IL-17 staining, further separated by expression of CD3 and NK1.1, and CD3+ IL-17+ cells were further distinguished based on expression of the γδ TCR and CD4.

(F and G) Representative FACS plots (F) and the graph (G) indicate the percentage of IL-17+ γδ TCR^{low} dermal γδ T cells in skin of WT and IL-38 KO mice at day 3.

(H and I) Representative FACS plots (H) and the graph (I) indicate the percentage of $CD11b^{+}$ $Ly6G^{+}$ neutrophils in skin of WT and IL-38 KO mice at day 5.

(J) DAPI-stained skin sections at day 6 (representative of five animals each) indicate microabscesses (red arrowheads). Scale bars represent 200 μm.

(K) PhenOptics images of skin sections from 6-day IMQ-treated mice (representative of five animals each) stained with anti-Ki67 (blue), anti-Keratin14 (green), anti-Keratin10 (yellow), anti-involucrin (violet), anti-loricrin (red), and DAPI (white). Scale bars represent 80 μm.

(L) Keratin10 expression in WT and IL-38 KO mouse skin treated with IMQ for the times indicated was analyzed by western blot. Glyceraldehyde-3-phosphate dehydrogenase (GAPDH) was the loading control. A representative western blot out of six independent experiments and the quantification are shown. Data are means ± SEM.

All data are biological replicates. *$p < 0.05$; **$p < 0.01$; ***$p < 0.001$; p values were calculated using a Mann-Whitney test (A, C, D, G, and I) or two-way ANOVA with Bonferroni's correction (L).

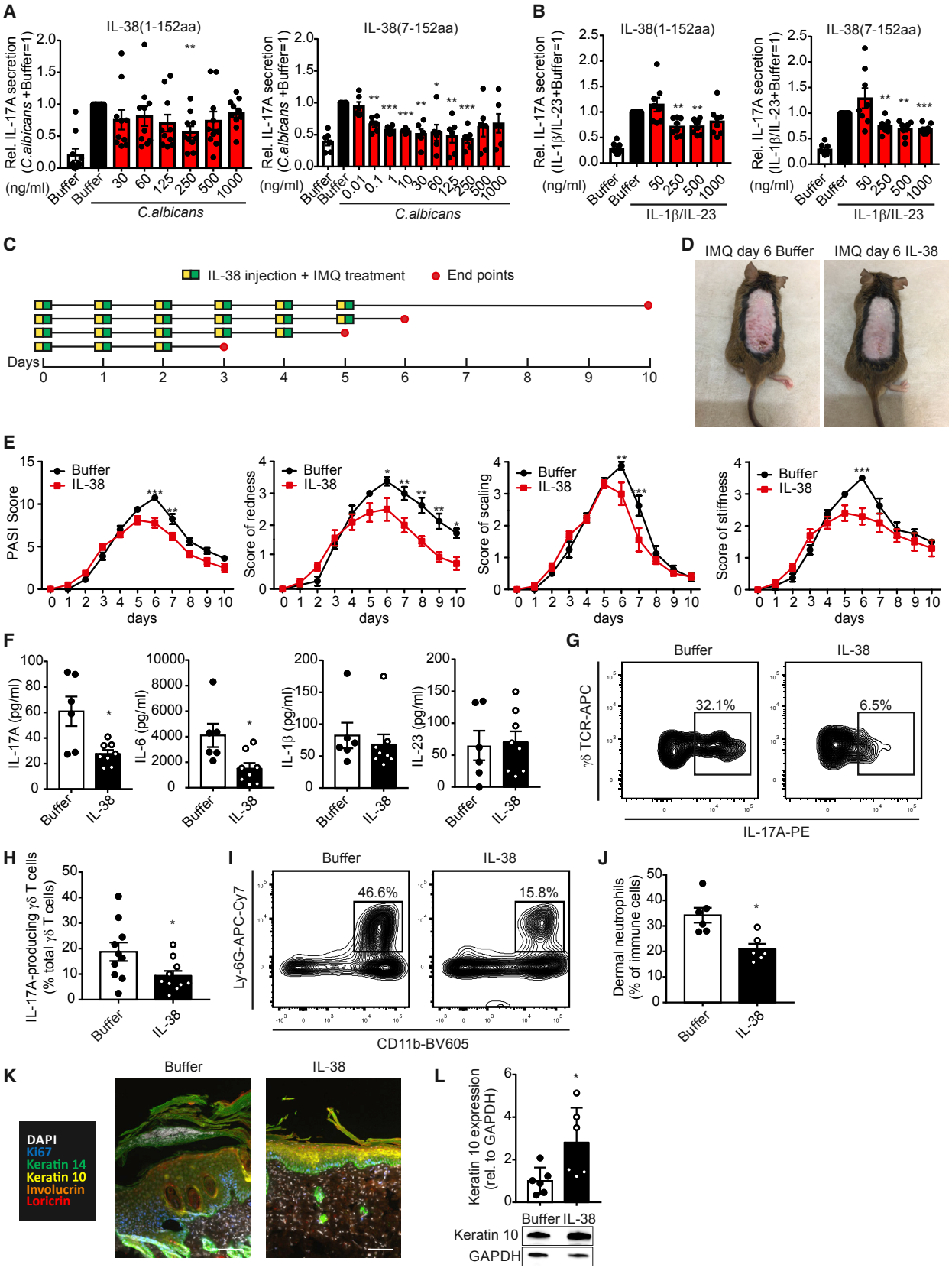

(legend on next page)

IL-38 (aa 7–152) (Figures S5A and S5B). Those variants were tested for their ability to decrease IL-17 production in human and murine *in vitro* models. IL-17 production induced by *C. albicans* in human PBMCs (Sutton et al., 2009; van de Veerdonk et al., 2012) was reduced by full-length IL-38 only at a concentration of 250 ng/mL, whereas mature IL-38 limited IL-17 production at a much broader concentration range, from 100 pg/mL to 250 ng/mL (Figure 3A). Other variants were less effective than mature IL-38 (Figures S5B and S5C). Since human and mouse IL-38 share 82.1% amino-acid sequence identity, we tested whether human IL-38 constructs were suitable for use in mice. Mouse spleen cells were stimulated with IL-1β and IL-23 on anti-CD3-coated plates to induce IL-17 production. In this setup, IL-17 secretion was significantly inhibited by both full-length and mature constructs (Figure 3B), while the marked difference in efficacy of human mature versus full-length IL-38 was blunted. Nevertheless, we subcutaneously injected mature IL-38 into the lower back skin of IL-38 KO mice daily before IMQ application for up to 6 days, followed by a 4-day observation period (Figure 3C). PASI scores of IL-38-injected mice were markedly improved compared to those of control mice (Figures 3D and 3E). Skin redness was decreased after day 6, scaling was reduced at day 6 and day 7, and stiffness was suppressed at day 6 (Figure 3E). Along with the phenotype changes, protein levels of IL-17A and IL-6 at day 3 were significantly reduced upon IL-38 injection, whereas IL-1β and IL-23 protein levels were not altered (Figure 3F). Importantly, IL-38 injection inhibited IL-17A production by dermal γδ T cells (Figures 3G and 3H). Along with reduced IL-17A levels, dermal neutrophil infiltration was significantly reduced after 5 consecutive days of IL-38 injection (Figures 3I and 3J). Finally, keratinocyte differentiation markers—in particular, Krt10 expression—were increased in IL-38-treated psoriatic animals compared to control animals, indicating recovery of skin regeneration (Figures 3K and 3L). Interestingly, application of mature IL-38 to IMQ-treated WT mice mildly reduced PASI scores, which was solely based on decreased scaling but not inflammation (Figure S6). These data may indicate that decreased IL-38 expression levels in WT mice during IMQ-induced psoriasis were still sufficient to limit γδ T cell activation. However, the beneficial effect of IL-38 on keratinocyte differentiation may require higher IL-38 concentrations, which is suggested by the reduced scaling in WT mice upon IL-38 injection (Figure S6).

Anti-γδ TCR Antibodies Limit γδ T Cell IL-17 Production in IL-38 KO Mice

Activation of γδ T cells occurs via innate (e.g., via cytokines) and adaptive (via the TCR) mechanisms. Supplementing IL-38 KO mice with IL-38 limited IL-17A production by dermal γδ T cells but did not restrict levels of the major γδ T17-activating cytokines IL-1β and IL-23 (Sutton et al., 2009). Therefore, we questioned whether IL-38 might directly act on γδ T cells to suppress IL-17 production. To answer this question, we established an *in vitro* γδ T cell activation assay using splenic γδ T cells. We used splenic γδ T cells mainly to be able to FACS (fluorescence-activated cell sorting)-sort a sufficient number of cells. Splenic and dermal γδ T cells show differences concerning TCR composition, (pre-)activation state, and cytokine output upon stimulation (O'Brien and Born, 2015). Previous work established an important role for dermal Vγ4+ γδ T cells in IL-17 production during skin inflammation (Cai et al., 2011). The same study also identified splenic Vγ4+ γδ T cells that produce IL-17 (Cai et al., 2011). Based on these findings, we deemed splenic γδ T cells as a suitable model to study γδ T cell IL-17 production, although a direct transfer of findings obtained with splenic γδ T cells to dermal γδ T cells cannot be made. We isolated γδ T cells from the spleens of WT mice and stimulated them with IL-1β and IL-23 after seeding them on plates coated with or without anti-CD3 antibody, which serves to mimic TCR stimulation (Figures 4A and 4B). IL-17 production was measured after 4 days alone or in combination with increasing concentrations of IL-38, IL-1RA, and IL-36RA. As expected, IL-1β and IL-23 induced IL-17 production at lower levels in the absence (Figure 4B), compared to the presence, of the anti-CD3 antibody (Figure 4B). In both cases, IL-36RA had no effect on IL-17 production. As expected when using IL-1β as a stimulus, IL-1RA

Figure 3. Mature IL-38 Inhibits Skin Inflammation

(A) Human PBMCs were stimulated with *Candida albicans* and serially diluted full-length IL-38 (1–152 aa) or mature IL-38 (7–152 aa) for 5 days. IL-17A production was analyzed using cytometric bead array (CBA). Data are means ± SEM of 10 or 6 individual donors, respectively (see also Figure S5).

(B) Mouse spleen cells were stimulated with IL-23/IL-1β and IL-38 (1–152 aa or 7–152 aa) at the concentrations indicated. IL-17A production was analyzed by CBA. Data are means ± SEM of 6 individual animals each.

(C–L) IL-38 KO mice received buffer or 1 mg/kg mature IL-38 subcutaneously (s.c.) and 62.5 mg IMQ on the back skin.

(C) The cartoon displays the experimental setup.

(D) Representative photographs of IL-38 KO mice (day 6) treated with buffer or mature IL-38.

(E) Cumulative Psoriasis Area Severity Index (PASI) scores and individual scores for redness, scaling, and stiffness are shown. Data are means ± SEM of five individual animals each, analyzed in two separate experiments.

(F) Cytokines on day 3 were determined by CBA. Data are means ± SEM of six (Buffer) or eight (IL-38) individual animals.

(G and H) Representative FACS plots (G) and the graph (H) indicate the percentage of IL-17A+ γδ TCR^{low} dermal γδ T cells at day 3. Data are means ± SEM of 10 individual animals each.

(I and J) Representative FACS plots (I) and the graph (J) indicate the percentage of $CD11b^+$ $Ly6G^+$ neutrophils at day 5. Data are means ± SEM of six individual animals each.

(K) Representative PhenOptics images of skin sections from 6-day IMQ-treated mice stained with anti-Ki67 (blue), anti-Keratin14 (green), anti-Keratin10 (yellow), anti-involucrin (orange), anti-loricrin (red), and DAPI (white). Scale bars represent 80 μm.

(L) Keratin10 expression in WT and IL-38 KO mouse skin at day 6 was analyzed by western blot. Glyceraldehyde-3-phosphate dehydrogenase (GAPDH) was the loading control. A representative western blot out of three independent experiments and the quantification are shown. Data are means ± SEM.

All data are biological replicates. *$p < 0.05$; **$p < 0.01$; ***$p < 0.001$; p values were calculated using one-sample t test (A and B), two-way ANOVA with Bonferroni's correction (E), or Mann-Whitney test (F, H, J, and L).

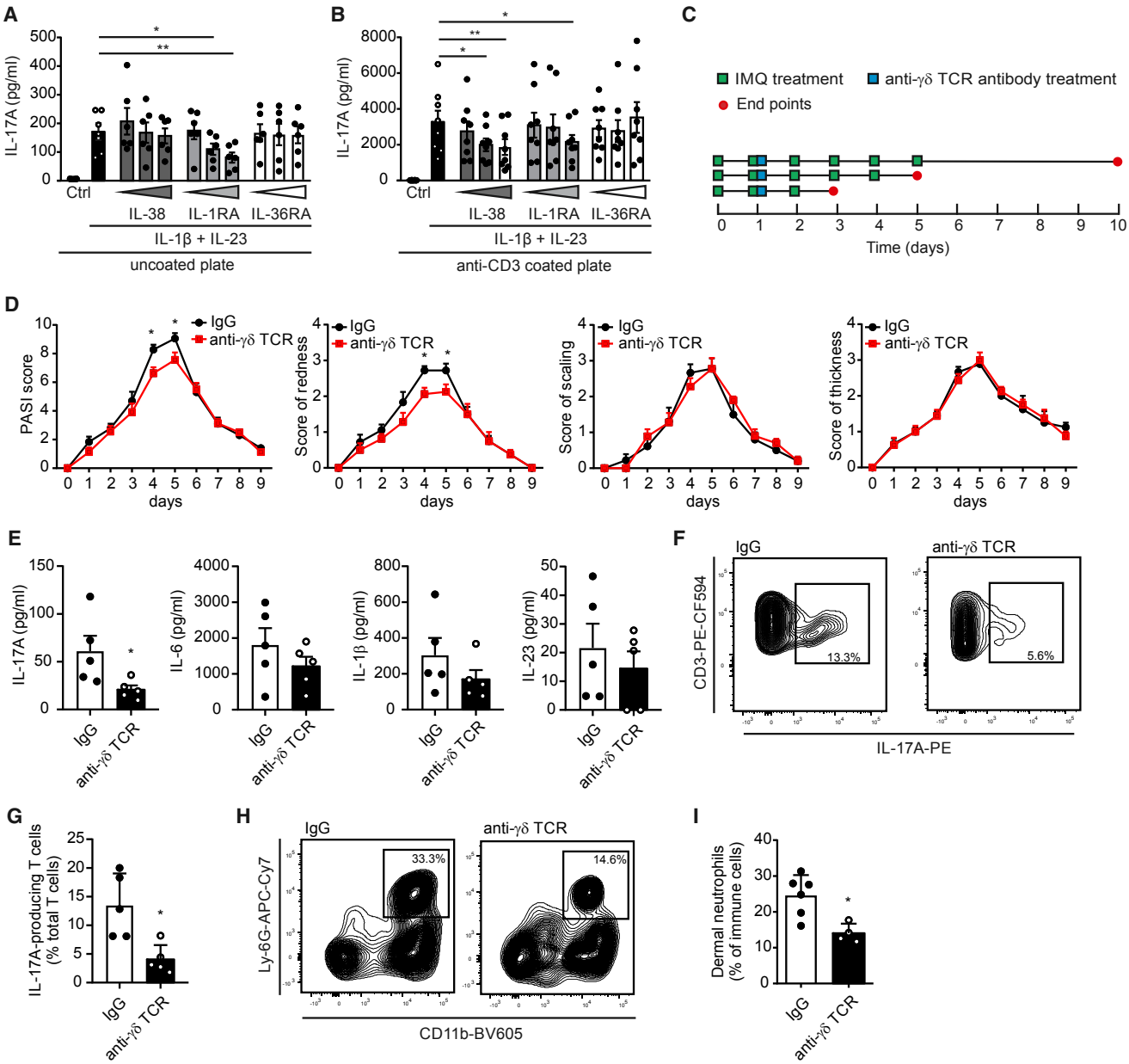

Figure 4. Anti-γδ TCR Antibodies Reduce Inflammation in Psoriatic IL-38 KO Mice

(A and B) FACS-sorted γδ T cells from wild-type mouse spleens were seeded on uncoated (A) and anti-CD3 antibody-coated (B) plates and stimulated with IL-1β (10 ng/mL) and IL-23 (10 ng/mL) in combination with increasing concentrations (10 ng/mL, 50 ng/mL, 100 ng/mL) of IL-38, IL-1RA, or IL-36RA. Data are means ± SEM of six (A) or eight (B) individual experiments.

(C–I) IL-38 KO mice received 62.5 mg IMQ on the back skin and a single 500-μg immunoglobulin G (IgG) control or anti-γδ TCR antibody application on day 1.

(C) The cartoon displays the experimental setup.

(D) Cumulative Psoriasis Area Severity Index (PASI) scores and individual scores for redness, scaling, and stiffness are shown. Data are means ± SEM of five individual animals each.

(E) Cytokines on day 3 were determined by CBA. Data are means ± SEM of five individual animals of each group.

(F and G) Representative FACS plots (F) and the graph (G) show the percentage of IL-17A+ T cells at day 3. Data are means ± SEM of five individual animals each.

(H and I) Representative FACS plots (H) and the graph (I) show percentage of $CD11b^+$ $Ly6G^+$ neutrophils at day 5. Data are means ± SEM of six (IgG) or four (anti-γδ TCR) individual animals.

All data are biological replicates. *$p < 0.05$; p values were calculated using a paired t test (A and B), two-way ANOVA with Bonferroni's correction (D), or Mann-Whitney test (E, G, and I).

dose-dependently inhibited IL-17 production in the absence and presence of the anti-CD3 antibody, although efficacy was reduced when γδ T cells were seeded on anti-CD3 antibody-coated plates (Figures 4A and 4B). Interestingly, IL-38 treatment had no effect on IL-17 production in the absence of a TCR stimulus but showed a dose-dependent inhibition of IL-17 production in anti-CD3-stimulated γδ T cells (Figures 4A and 4B). To further substantiate that IL-38 affects γδ T cell activation in response to TCR activation, we used a γδ TCR blocking antibody, which does not deplete γδ T cells but rather blocks TCR signaling (Koenecke et al., 2009), in the IMQ-induced psoriasis model in IL-38 KO mice (Figure 4C). The γδ TCR blocking antibody reduced PASI scores at days 4 and 5 in IL-38 KO mice compared with the isotype control, which was entirely based on reducing redness, while scaling and stiffness were unaltered (Figure 4D). Accordingly, the γδ TCR blocking antibody significantly reduced the levels of IL-17A at day 3, but not of other cytokines, and limited IL-17 production from T cells (Figures 4E–4G). Investigating IL-17A production specifically from γδ T cells was not possible in this setting, since the neutralizing antibody masks the epitope for the FACS antibody used to identify γδ T cells. Moreover, dermal neutrophil infiltrates were reduced at day 5 (Figures 4H and 4I), which correlated with reduced redness. Together, these data indicate that increased inflammation, rather than alterations in keratinocyte differentiation, in IL-38 KO mice was reverted by blocking the γδ TCR.

IL1RAPL1 Promotes γδ T Cell IL-17 Production *In Vitro*

IL-38, but not IL-36RA, affected IL-17 production by anti-CD3 antibody-activated γδ T cells, and IL-38 was ineffective in samples without anti-CD3 antibody, a scenario in which IL-1RA was effective (Figures 4A and 4B). Thus, IL-38 likely inhibited IL-17 release, at least not primarily, via IL-1R and IL-36R. Beside these receptors, IL-38 may act as an antagonist of IL1RAPL1 (Mora et al., 2016). IL1RAPL1 is mainly expressed in the CNS at baseline. However, we observed basal IL1RAPL1 expression on γδ T cells, which was increased time-dependently at day 3 after anti-CD3 stimulation, both at the mRNA and protein levels (Figures 5A–5C). In contrast, IL1RAPL1 was not increased in CD4+ T cells upon *in vitro* activation with anti-CD3 and TH17-promoting cytokines (Figure S7A). Increased IL1RAPL1 expression by γδ T cells was required for maximal IL-17 production *in vitro*, since IL1RAPL1 KO γδ T cells produced lower levels of IL-17 compared to their WT counterparts (Figure 5D). When looking at IL-17 release kinetics, IL17 levels were increased in WT γδ T cells between day 3 and day 4 (Figure 5D), accompanied by increased expression of the TH17 and γδ T17 transcription factor Rorc (Figures 5D and 5E). Both features were decreased in IL1RAPL1 KO γδ T cells (Figures 5D and 5E), indicating a role for IL1RAPL1 in feedforward production of IL-17. Release of other cytokines such as IL-6 and IFN-γ was not decreased in IL1RAPL1 KO γδ T cells (Figure S7B). Importantly, IL-38 was unable to block IL-17 production in the absence of IL1RAPL1 (Figure 5F). These data may indicate that IL-38 suppresses IL-17 release from γδ T cells, at least partly, via IL1RAPL1. To substantiate this claim, we used competition and receptor binding assays to show a direct interaction between IL-38 and IL1RAPL1 in the murine system. We induced IL1RAPL1 expression on spleen γδ T cells by anti-CD3 stimulation and added recombinant mouse IL-38 before analyzing the surface expression of IL1RAPL1. IL-38 competed with the IL1RAPL1 antibody in FACS analysis, giving a first indication that IL-38 may bind to IL1RAPL1 on spleen γδ T cells (Figures 5G and 5H). To substantiate this finding, we performed a receptor binding assay using murine IL1RAPL1-Fc chimera-coated plates incubated with increasing concentrations of in-house-generated recombinant mouse IL-38. We observed the binding of IL-38 to mouse IL1RAPL1 compared to the BSA control, with similar kinetics when compared to the human proteins (Figure 5I), which we have previously reported (Mora et al., 2016).

IL1RAPL1 KO Limits IL-17 Production by Dermal γδ T Cells

To analyze the contribution of IL1RAPL1 to dermal γδ T cell activation *in vivo*, we subjected WT and IL1RAPL1 KO mice to IMQ-induced psoriasis. IL1RAPL1 KO mice showed reduced PASI scores at day 5 compared to those of WT mice, which was mainly attributable to reduced redness; i.e., inflammation (Figure 6A). In association with reduced inflammation, the production of IL-17 from dermal γδ T cells decreased in psoriatic IL1RAPL1 KO skin on day 3 (Figures 6B and 6C), which correlated with attenuated overall IL-17 levels (Figure 6D). Other inflammatory cytokines, including IL-6, IL-1β, and IL-23, also showed a trend toward or a significant decrease in psoriatic IL1RAPL1 KO compared to WT skin (Figure 6D). IL-38 levels were not significantly altered in IL1RAPL1 KO compared to WT mice during IMQ-induced psoriasis (Figure 6E), despite a trend toward slightly increased IL-38 levels at baseline, indicating that IL1RAPL1 KO did not affect dermal γδ T cell activation in the IMQ model by increasing IL-38 expression. The role of IL1RAPL1 in γδ T cell activation in psoriasis is substantiated by an expression correlation of IL1RAPL1 with the γδ T cell-enriched transcription factor ZBTB16 and the γδ T17-enriched chemokine receptor CCR6 in the skin of psoriasis patients (Figures 6F and 6G). Overall, these data suggest that IL-38 limits IL-17 production from γδ T cells, which requires the presence of IL1RAPL1. IL1RAPL1, in turn, is required for optimal IL-17 production from γδ T cells both *in vitro* and in the IMQ-induced psoriasis mouse model.

DISCUSSION

Our study identifies a mechanism by which IL-38 restricts IL-17-driven inflammation. IL-38 directly inhibits the activation of γδ T cells, which may occur by antagonizing IL1RAPL1. IL1RAPL1 is upregulated on γδ T cells upon TCR activation (mimicked by anti-CD3 antibodies) to serve as a feedforward amplifier of IL-17 production. In this regard, IL1RAPL1 meets the requirements of a stimulatory immune checkpoint (Pardoll, 2012). It is expressed at low levels in unstimulated immune cells but is upregulated upon activation in γδ T cells (Figures 5A–5C) and macrophages (Mora et al., 2016). Moreover, its upregulation is required to achieve the maximal response to the stimulus that induces IL1RAPL1 upregulation itself. IL1RAPL1 induction appears to specifically promote IL-17 generation, as indicated in our study here and before (Mora et al., 2016). Therefore,

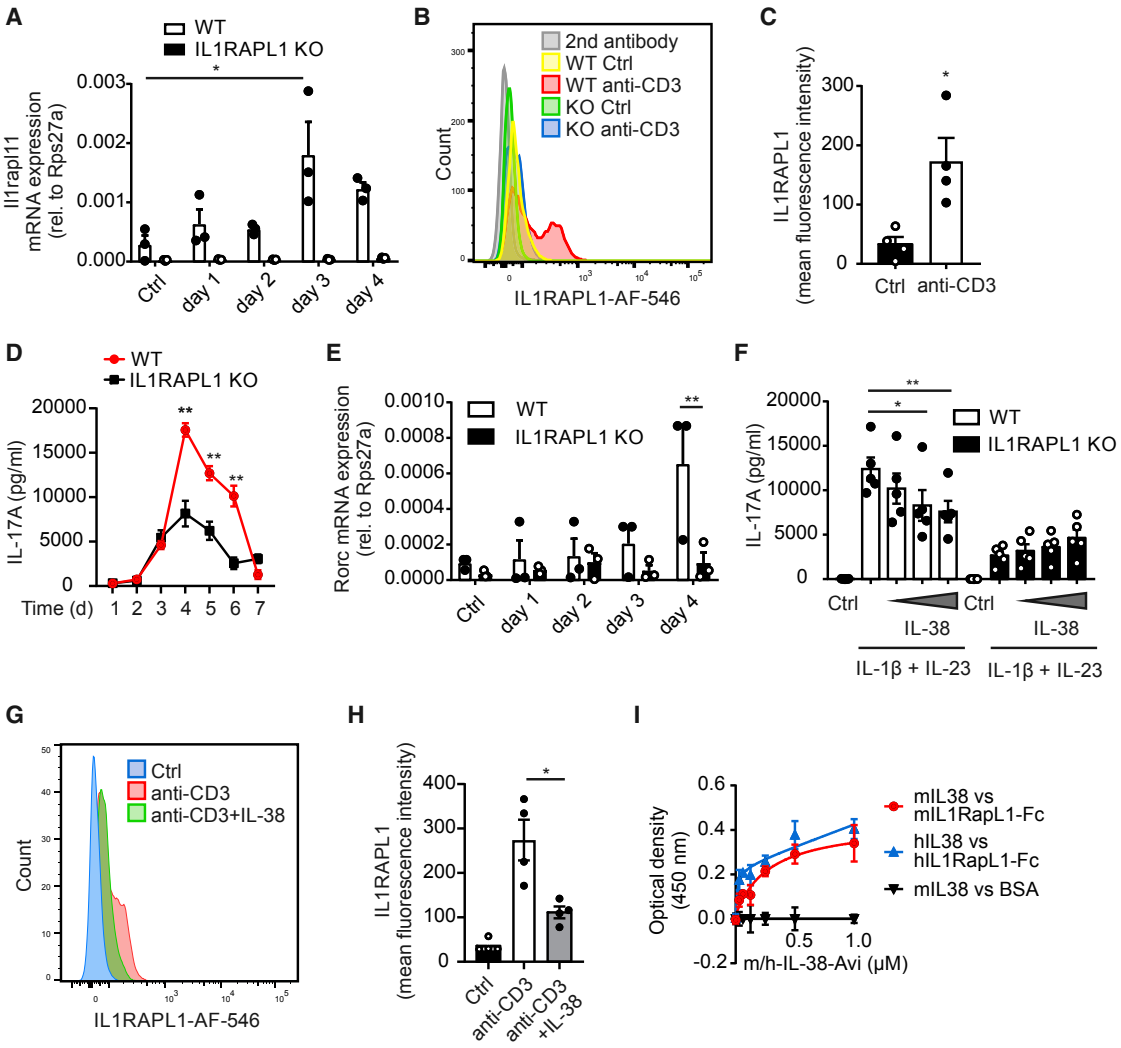

Figure 5. IL-38 Blocks IL-17 Production by γδ T Cells in the Presence of IL-1RAPL1

(A–F) FACS-sorted γδ T cells from wild-type or X-linked interleukin-1 receptor accessory protein-like 1 (IL1RAPL1) KO mouse spleens were seeded on anti-CD3 antibody-coated plates and stimulated with IL-1β (10 ng/mL) and IL-23 (10 ng/mL) with or without increasing concentrations (10 ng/mL, 50 ng/mL, and 100 ng/mL) of IL-38 for the times indicated.

(A) Il1rapl1 mRNA expression was determined by qPCR at the times indicated. Data are means ± SEM of three individual animals each.

(B and C) Cell surface expression of IL1RAPL1 on γδ T cells was determined by flow cytometry. Representative histograms (B) and the quantification (C) at day 3 are shown. Data are means ± SEM of seven individual animals each.

(D) IL-17A levels at the times indicated were determined by CBA. Data are means ± SEM of six individual animals each.

(E) Rorc mRNA expression was determined by qPCR at the times indicated. Data are means ± SEM of three individual animals each.

(F) IL-17A levels at day 4 were determined by CBA. Data are means ± SEM of five individual animals each.

(G and H) FACS-sorted γδ T cells from wild-type spleens were controls or stimulated with anti-CD3 antibodies for 3 days. 50 ng/mL IL-38 or the vehicle controls was added for 15 min on ice before staining with anti-IL1RAPL1 antibody. Representative histograms (G) and the quantification (H) are shown. Data are means ± SEM of four individual animals.

(I) Binding kinetics of Avi-tagged mouse (red) or human (blue) IL-38 to immobilized mouse or human IL1RAPL1, respectively, are shown. Plates were coated with 0.1 μg per well of IL1RAPL1/Fc chimera and incubated with increasing amounts of recombinant IL-38 as indicated. IL-38 binding to the extracellular domain of IL1RAPL1 was detected using NeutrAvidin-HRP.

All data are biological replicates, with the exception of the data in (I), were three technical replicates of a representative experiment are shown. *$p < 0.05$; **$p < 0.01$; ***$p < 0.001$; p values were calculated using a Mann-Whitney test (C–F), Kruskal-Wallis test with Dunn's correction (A), or two-way ANOVA with Bonferroni's correction (D and E).

IL1RAPL1 might be a target to interfere with IL-17 production in humans suffering from diseases with a proven IL-17-driven etiology, such as psoriasis (Nestle et al., 2009; Reich et al., 2015).

A lack of effect of IL-38 KO in IMQ skin inflammation was found by others in a different mouse strain. In this study, IMQ-induced inflammation in the ear and tail skin in BALB/c mice

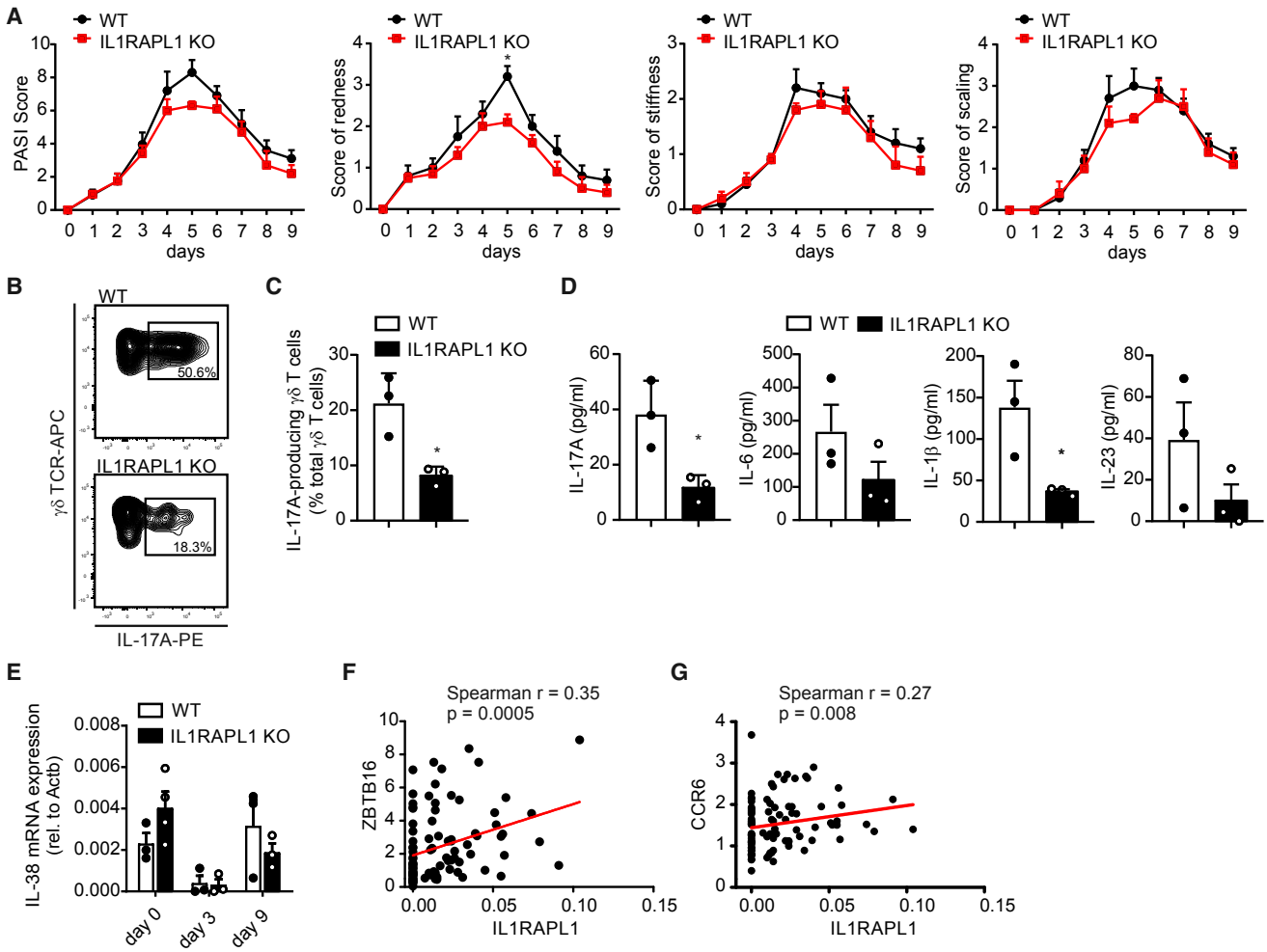

Figure 6. Reduced IL-17 Production by γδ T Cells in IL1RAPL1 KO Mice

(A–E) WT and IL1RAPL1 KO mice were treated daily with 62.5 mg IMQ on the back skin.

(A) Cumulative Psoriasis Area Severity Index (PASI) scores and individual scores for redness, scaling, and stiffness are shown. Data are means ± SEM of five individual animals each.

(B and C) Representative FACS plots (B) and the graph (C) show the percentage of IL-17A+ γδ TCR^{low} dermal γδ T cells at day 3. Data are means ± SEM of three individual animals each.

(D) Cytokines on day 3 were determined by CBA. Data are means ± SEM of three individual animals of each group.

(E) IL-38 mRNA expression in psoriatic WT and IL1RAPL1 KO skin was quantified at the times indicated. Data are means ± SEM of at least three individual animals each.

(F and G) Publicly available data from human psoriasis patients (Li et al., 2014a) were analyzed to correlate the expression of IL1RAPL1 with the γδ T cell-enriched transcription factor ZBTB16 (F) and the γδ T17-enriched chemokine receptor CCR6 (G).

All data are biological replicates. *p < 0.05; p values were calculated using an unpaired t test in (C) and (D) or two-way ANOVA with Bonferroni's correction in (A).

was investigated (Palomo et al., 2018). Also in our strain, ear skin inflammation was not altered in IL-38 KO mice (data not shown). The fact that—in comparison to the anatomically less specialized back skin—ear and tail skin contains significantly fewer T cells (Tong et al., 2015) rather supports our finding that exacerbated IMQ-induced skin in IL-38 KO mice depends on γδ T cells. Importantly, psoriasis in humans rarely involves the ears. While this study was under revision, a paper was published showing that IL-38 applied to the back skin of BALB/c mice in the IMQ model reduced disease severity (Mercurio et al., 2018). The authors showed that IL-38 directly promotes keratinocyte differentiation *in vitro*, independent of regulating inflammation. We also observed that the lack of IL-38 negatively affects keratinocyte differentiation in the IMQ model, which is reversed upon re-supplementation. We currently cannot distinguish whether altered IL-38 concentrations in our study regulated keratinocyte differentiation through modifying inflammation. However, IL-38 promoted keratinocyte differentiation in IMQ-treated WT mice in the study of Mercurio et al. (2018). BALB/c mice that were used in that study did not produce significant IL-17 levels in the IMQ model, compared to C57BL/6 mice (Swindell et al., 2017). Therefore, IL-38 can promote

keratinocyte differentiation independently of at least IL-17-driven inflammation, which is further substantiated by our finding that a γδ TCR blocking antibody reduced inflammation, but not scaling, in IL-38 KO mice.

Our study suggests mature IL-38 as a potential treatment option for patients suffering from IL-17-driven disease. IL-38 was only mildly effective in psoriatic WT mice, which might be due to the remaining high endogenous IL-38 levels in the skin that are sufficient to affect γδ T cell activation. Inflammatory reactions in tissues with low endogenous IL-38 expression might, therefore, be better targets for therapy with mature recombinant human IL-38, which is supported by the anti-inflammatory effect of IL-38 overexpression in murine arthritis models (Boutet et al., 2017). A benefit of IL-38 would be its potential to target more than one receptor of the IL-1 family and to interfere with more than one cytokine involved in chronic inflammation, including IL-6, IL-17, and TNF-α (Boraschi et al., 2018; Tabas and Glass, 2013). This may circumvent inherent drawbacks of current innovative anti-inflammatory drugs such as redundancy and compensation within the inflammatory process, which can lead to therapy resistance as described for TNF-α targeting agents (Emery et al., 2008). Mature IL-38 appears to be superior in a treatment scenario, given its efficacy at a broader concentration range compared to full-length IL-38. In this aspect, IL-38 shows a remarkable similarity to IL-37, another anti-inflammatory IL-1 family protein. In the case of IL-37, processing prevents homo-dimerization to increase biological activity (Ellisdon et al., 2017). Whether a similar mechanism applies to IL-38 remains to be tested.

STAR★METHODS

Detailed methods are provided in the online version of this paper and include the following:

- KEY RESOURCES TABLE
- CONTACT FOR REAGENT AND RESOURCE SHARING
- EXPERIMENTAL MODEL AND SUBJECT DETAILS
  - Psoriasisform dermatitis model
- METHOD DETAILS
  - Flow cytometry and cell sorting
  - RNA extraction and quantitative real-time PCR
  - Western Blotting
  - Production of human recombinant IL-38 variants
  - *In vitro* immune cell activation assays
  - Cytometric Bead Array
  - Immunohistochemistry
  - Expression and purification of mouse recombinant IL38
  - Receptor binding assay
  - Analysis of publicly available human datasets
- QUANTIFICATION AND STATISTICAL ANALYSIS

SUPPLEMENTAL INFORMATION

Supplemental Information can be found online at https://doi.org/10.1016/j.celrep.2019.03.082.

ACKNOWLEDGMENTS

The authors thank Margarethe Mijatovic and Praveen Mathoor for excellent technical assistance. We are grateful to Johannes Buyel, Dirk Scheffler, Robin Kastilan, and Michael Limberg for large-scale protein production at the Fraunhofer Institute IME, Aachen, Germany. The authors are supported by the Else Kroner-Fresenius Foundation (EKFS), Deutsche Krebshilfe (70112451), the Landesoffensive zur Entwicklung wissenschaftlich-ökonomischer Exzellenz (LOEWE; LOEWE Center for Translational Medicine and Pharmacology), and Deutsche Forschungsgemeinschaft (DFG; GRK2336, SFB1039, and FOR2438). Y.H. was supported by the China Scholarship Council (CSC).

AUTHOR CONTRIBUTIONS

Conceptualization, J.M., H.B., M.J.P., A.E., B.B., and A.W; Methodology, Y.H., S.W., M.P., A.H., P.d.S., A.S., E.E., and N.d.B.; Formal Analysis, S.W., A.S., T. Schmid, A.E., and A.W.; Investigation, Y.H., J.M., M.P., A.H., P.d.S., S.W., C. Schuster, E.E., G.L., T. Scholz, N.d.B., and A.W.; Resources, P.B. and C. Sala; Data Curation, A.S., T. Schmid, and A.W.; Writing – Original Draft, Y.H., J.M., and A.W.; Writing – Review & Editing, all authors; Visualization, Y.H., J.M., and A.W.; Supervision, M.J.P., A.E., B.B., and A.W.; Funding Acquisition, M.J.P., A.E., B.B., and A.W.

DECLARATION OF INTERESTS

The authors declare no competing interests.

Received: July 2, 2018
Revised: March 4, 2019
Accepted: March 21, 2019
Published: April 16, 2019

REFERENCES

Barrett, T., Wilhite, S.E., Ledoux, P., Evangelista, C., Kim, I.F., Tomashevsky, M., Marshall, K.A., Phillippy, K.H., Sherman, P.M., Holko, M., et al. (2013). NCBI GEO: archive for functional genomics data sets—update. Nucleic Acids Res. *41*, D991–D995.

Blumberg, H., Dinh, H., Dean, C., Jr., Trueblood, E.S., Bailey, K., Shows, D., Bhagavathula, N., Aslam, M.N., Varani, J., Towne, J.E., and Sims, J.E. (2010). IL-1RL2 and its ligands contribute to the cytokine network in psoriasis. J. Immunol. *185*, 4354–4362.

Boraschi, D., Italiani, P., Weil, S., and Martin, M.U. (2018). The family of the interleukin-1 receptors. Immunol. Rev. *281*, 197–232.

Boutet, M.A., Bart, G., Penhoat, M., Amiaud, J., Brulin, B., Charrier, C., Morel, F., Lecron, J.C., Rolli-Derkinderen, M., Bourreille, A., et al. (2016). Distinct expression of interleukin (IL)-36α, β and γ, their antagonist IL-36Ra and IL-38 in psoriasis, rheumatoid arthritis and Crohn's disease. Clin. Exp. Immunol. *184*, 159–173.

Boutet, M.A., Najm, A., Bart, G., Brion, R., Touchais, S., Trichet, V., Layrolle, P., Gabay, C., Palmer, G., Blanchard, F., and Le Goff, B. (2017). IL-38 overexpression induces anti-inflammatory effects in mice arthritis models and in human macrophages in vitro. Ann. Rheum. Dis. *76*, 1304–1312.

Cai, Y., Shen, X., Ding, C., Qi, C., Li, K., Li, X., Jala, V.R., Zhang, H.G., Wang, T., Zheng, J., and Yan, J. (2011). Pivotal role of dermal IL-17-producing γδ T cells in skin inflammation. Immunity *35*, 596–610.

Chu, M., Tam, L.S., Zhu, J., Jiao, D., Liu, H., Cai, Z., Dong, J., Kai Lam, C.W., and Wong, C.K. (2017). In vivo anti-inflammatory activities of novel cytokine IL-38 in Murphy Roths Large (MRL)/lpr mice. Immunobiology *222*, 483–493.

Ellisdon, A.M., Nold-Petry, C.A., D'Andrea, L., Cho, S.X., Lao, J.C., Rudloff, I., Ngo, D., Lo, C.Y., Soares da Costa, T.P., Perugini, M.A., et al. (2017). Homodimerization attenuates the anti-inflammatory activity of interleukin-37. Sci. Immunol. *2*, eaaj1548.

Emery, P., Keystone, E., Tony, H.P., Cantagrel, A., van Vollenhoven, R., Sanchez, A., Alecock, E., Lee, J., and Kremer, J. (2008). IL-6 receptor inhibition with tocilizumab improves treatment outcomes in patients with rheumatoid arthritis refractory to anti-tumour necrosis factor biologicals: results from a 24-week multicentre randomised placebo-controlled trial. Ann. Rheum. Dis. *67*, 1516–1523.

Guo, Z.S., Li, C., Lin, Z.M., Huang, J.X., Wei, Q.J., Wang, X.W., Xie, Y.Y., Liao, Z.T., Chao, S.Y., and Gu, J.R. (2010). Association of IL-1 gene complex members with ankylosing spondylitis in Chinese Han population. Int. J. Immunogenet. *37*, 33–37.

Jung, M.Y., Kang, S.W., Kim, S.K., Kim, H.J., Yun, D.H., Yim, S.V., Hong, S.J., and Chung, J.H. (2010). The interleukin-1 family gene polymorphisms in Korean patients with rheumatoid arthritis. Scand. J. Rheumatol. *39*, 190–196.

Koenecke, C., Chennupati, V., Schmitz, S., Malissen, B., Förster, R., and Prinz, I. (2009). In vivo application of mAb directed against the gammadelta TCR does not deplete but generates "invisible" gammadelta T cells. Eur. J. Immunol. *39*, 372–379.

Li, B., Tsoi, L.C., Swindell, W.R., Gudjonsson, J.E., Tejasvi, T., Johnston, A., Ding, J., Stuart, P.E., Xing, X., Kochkodan, J.J., et al. (2014a). Transcriptome analysis of psoriasis in a large case-control sample: RNA-seq provides insights into disease mechanisms. J. Invest. Dermatol. *134*, 1828–1838.

Li, N., Yamasaki, K., Saito, R., Fukushi-Takahashi, S., Shimada-Omori, R., Asano, M., and Aiba, S. (2014b). Alarmin function of cathelicidin antimicrobial peptide LL37 through IL-36γ induction in human epidermal keratinocytes. J. Immunol. *193*, 5140–5148.

Lin, H., Ho, A.S., Haley-Vicente, D., Zhang, J., Bernal-Fussell, J., Pace, A.M., Hansen, D., Schweighofer, K., Mize, N.K., and Ford, J.E. (2001). Cloning and characterization of IL-1HY2, a novel interleukin-1 family member. J. Biol. Chem. *276*, 20597–20602.

Martin, B., Hirota, K., Cua, D.J., Stockinger, B., and Veldhoen, M. (2009). Interleukin-17-producing gammadelta T cells selectively expand in response to pathogen products and environmental signals. Immunity *31*, 321–330.

Mercurio, L., Morelli, M., Scarponi, C., Eisenmesser, E.Z., Doti, N., Pagnanelli, G., Gubinelli, E., Mazzanti, C., Cavani, A., Ruvo, M., et al. (2018). IL-38 has an anti-inflammatory action in psoriasis and its expression correlates with disease severity and therapeutic response to anti-IL-17A treatment. Cell Death Dis. *9*, 1104.

Mora, J., Schlemmer, A., Wittig, I., Richter, F., Putyrski, M., Frank, A.C., Han, Y., Jung, M., Ernst, A., Weigert, A., and Brüne, B. (2016). Interleukin-38 is released from apoptotic cells to limit inflammatory macrophage responses. J. Mol. Cell Biol., mjw006.

Nestle, F.O., Kaplan, D.H., and Barker, J. (2009). Psoriasis. N. Engl. J. Med. *361*, 496–509.

O'Brien, R.L., and Born, W.K. (2015). Dermal γδ T cells–what have we learned? Cell. Immunol. *296*, 62–69.

Palomo, J., Troccaz, S., Talabot-Ayer, D., Rodriguez, E., and Palmer, G. (2018). The severity of imiquimod-induced mouse skin inflammation is independent of endogenous IL-38 expression. PLoS ONE *13*, e0194667.

Pardoll, D.M. (2012). The blockade of immune checkpoints in cancer immunotherapy. Nat. Rev. Cancer *12*, 252–264.

Pavlowsky, A., Gianfelice, A., Pallotto, M., Zanchi, A., Vara, H., Khelfaoui, M., Valnegri, P., Rezai, X., Bassani, S., Brambilla, D., et al. (2010). A postsynaptic signaling pathway that may account for the cognitive defect due to IL1RAPL1 mutation. Curr. Biol. *20*, 103–115.

Rabeony, H., Petit-Paris, I., Garnier, J., Barrault, C., Pedretti, N., Guilloteau, K., Jegou, J.F., Guillet, G., Huguier, V., Lecron, J.C., et al. (2014). Inhibition of keratinocyte differentiation by the synergistic effect of IL-17A, IL-22, IL-1α, TNFα and oncostatin M. PLoS ONE *9*, e101937.

Rahman, P., Sun, S., Peddle, L., Snelgrove, T., Melay, W., Greenwood, C., and Gladman, D. (2006). Association between the interleukin-1 family gene cluster and psoriatic arthritis. Arthritis Rheum. *54*, 2321–2325.

Reich, K., Papp, K.A., Matheson, R.T., Tu, J.H., Bissonnette, R., Bourcier, M., Gratton, D., Kunynetz, R.A., Poulin, Y., Rosoph, L.A., et al. (2015). Evidence that a neutrophil-keratinocyte crosstalk is an early target of IL-17A inhibition in psoriasis. Exp. Dermatol. *24*, 529–535.

Rudloff, I., Godsell, J., Nold-Petry, C.A., Harris, J., Hoi, A., Morand, E.F., and Nold, M.F. (2015). Brief report: Interleukin-38 exerts antiinflammatory functions and is associated with disease activity in systemic lupus erythematosus. Arthritis Rheumatol. *67*, 3219–3225.

Sims, A.M., Timms, A.E., Bruges-Armas, J., Burgos-Vargas, R., Chou, C.T., Doan, T., Dowling, A., Fialho, R.N., Gergely, P., Gladman, D.D., et al.; International Genetics of Ankylosing Spondylitis (2008). Prospective meta-analysis of interleukin 1 gene complex polymorphisms confirms associations with ankylosing spondylitis. Ann. Rheum. Dis. *67*, 1305–1309.

Sutton, C.E., Lalor, S.J., Sweeney, C.M., Brereton, C.F., Lavelle, E.C., and Mills, K.H. (2009). Interleukin-1 and IL-23 induce innate IL-17 production from gammadelta T cells, amplifying Th17 responses and autoimmunity. Immunity *31*, 331–341.

Swindell, W.R., Michaels, K.A., Sutter, A.J., Diaconu, D., Fritz, Y., Xing, X., Sarkar, M.K., Liang, Y., Tsoi, A., Gudjonsson, J.E., and Ward, N.L. (2017). Imiquimod has strain-dependent effects in mice and does not uniquely model human psoriasis. Genome Med. *9*, 24.

Tabas, I., and Glass, C.K. (2013). Anti-inflammatory therapy in chronic disease: challenges and opportunities. Science *339*, 166–172.

Tong, P.L., Roediger, B., Kolesnikoff, N., Biro, M., Tay, S.S., Jain, R., Shaw, L.E., Grimbaldeston, M.A., and Weninger, W. (2015). The skin immune atlas: three-dimensional analysis of cutaneous leukocyte subsets by multiphoton microscopy. J. Invest. Dermatol. *135*, 84–93.

Towne, J.E., Renshaw, B.R., Douangpanya, J., Lipsky, B.P., Shen, M., Gabel, C.A., and Sims, J.E. (2011). Interleukin-36 (IL-36) ligands require processing for full agonist (IL-36α, IL-36β, and IL-36γ) or antagonist (IL-36Ra) activity. J. Biol. Chem. *286*, 42594–42602.

van de Veerdonk, F.L., Stoeckman, A.K., Wu, G., Boeckermann, A.N., Azam, T., Netea, M.G., Joosten, L.A., van der Meer, J.W., Hao, R., Kalabokis, V., and Dinarello, C.A. (2012). IL-38 binds to the IL-36 receptor and has biological effects on immune cells similar to IL-36 receptor antagonist. Proc. Natl. Acad. Sci. USA *109*, 3001–3005.

van de Veerdonk, F.L., de Graaf, D.M., Joosten, L.A., and Dinarello, C.A. (2018). Biology of IL-38 and its role in disease. Immunol. Rev. *281*, 191–196.

van der Fits, L., Mourits, S., Voerman, J.S., Kant, M., Boon, L., Laman, J.D., Cornelissen, F., Mus, A.M., Florencia, E., Prens, E.P., and Lubberts, E. (2009). Imiquimod-induced psoriasis-like skin inflammation in mice is mediated via the IL-23/IL-17 axis. J. Immunol. *182*, 5836–5845.

Weichand, B., Popp, R., Dziumbla, S., Mora, J., Strack, E., Elwakeel, E., Frank, A.C., Scholich, K., Pierre, S., Syed, S.N., et al. (2017). S1PR1 on tumor-associated macrophages promotes lymphangiogenesis and metastasis via NLRP3/IL-1β. J. Exp. Med. *214*, 2695–2713.

STAR★METHODS

KEY RESOURCES TABLE

REAGENT or RESOURCE	SOURCE	IDENTIFIER
Antibodies		
Anti-CD3e	BD Biosciences	Cat# 562286; RRID:AB_11153307
Anti-CD4	BD Biosciences	Cat# 560782; RRID:AB_1937315
Anti-CD4	BD Biosciences	Cat# 563050; RRID:AB_2737973
Anti-CD8a	Biolegend	Cat# 100742; RRID:AB_2563056
Anti-CD11b	Biolegend	Cat# 101257; RRID:AB_2565431
Anti-CD11c	BD Biosciences	Cat# 560583; RRID:AB_1727421
Anti-CD11c	BD Biosciences	Cat# 563048; RRID:AB_2734778
Anti-CD19	BD Biosciences	Cat# 560143; RRID:AB_1645234
Anti-CD45	Miltenyi	Cat# 130-102-430; RRID:AB_2659925
Anti-F4/80	Biolegend	Cat# 123114; RRID:AB_893478
Anti-HLA-DR (MHCII)	Miltenyi	Cat# 130-102-139; RRID:AB_2660058
Anti-Ly6C	BD Biosciences	Cat# 560525; RRID:AB_1727558
Anti-Ly6G	Biolegend	Cat# 127624; RRID:AB_10640819
Anti-SiglecH	Biolegend	Cat# 129604; RRID:AB_1227761
Anti-CD31	eBioscience	Cat# 25-0311-82; RRID:AB_2716949
Anti-CD90.2	Miltenyi	Cat# 130-102-960; RRID:AB_2659874
Anti-CD326	BD Biosciences	Cat# 563134; RRID:AB_2738022
Anti-GITR (CD357)	Biolegend	Cat# 126308; RRID:AB_1089125
Anti-NK1.1	BD Biosciences	Cat# 563096; RRID:AB_2738002
Anti-TCR γδ	Biolegend	Cat# 118116; RRID:AB_1731813
Anti-IFN-γ	BD Biosciences	Cat# 563376; RRID:AB_2738165
Anti-IL-17A	Biolegend	Cat# 506904; RRID:AB_315464
Anti-CD45	BD Biosciences	Cat# 560510; RRID:AB_1645208
InVivoMab anti-mouse TCR γ/δ	Bio XCell	Cat# BE0070; RRID:AB_1107751
InVivoMab polyclonal Armenian hamster IgG	Bio XCell	Cat# BE0091; RRID:AB_1107773
Anti-Ki67	Abcam	Cat# ab1667; RRID:AB_302459
Anti-Keratin10	Abcam	Cat# ab76318; RRID:AB_1523465
Anti-Keratin14	Biolegend	Cat# 905301; RRID:AB_2565048
Anti-Loricrin	Biolegend	Cat# 905101; RRID:AB_2565046
Anti-Involucrin	Biolegend	Cat# 924401; RRID:AB_2565452
Anti-IL1RAPL1	Proteintech	Cat# 21609-1-AP; RRID:AB_10888632
Chemicals, Peptides, and Recombinant Proteins		
FcR Blocking Reagent	Miltenyi Biotec	Cat# 130-092-575
Protein Transport Inhibitor	BD Biosciences	Cat# 554724
Brefeldin A (BFA)	Sigma Aldrich	Cat# B6542
Cell Stimulation Cocktail	eBioscience	Cat# 00-4970-93
Flow Cytometry Absolute Count Standard	Bangs Laboratories, Inc	Cat# 580
Brilliant Stain Buffer	BD Biosciences	Cat# 563794
Liberase TM Research Grade	Merck	Cat# 5401119001
DNase I, Bovine Pancreas	Merck	Cat# 260913-10MU
rmIL-23	Bio-Techne	Cat# 1 887 ML,O10
rmIL-1β	Bio-Techne	Cat# 401-ML-005
rm-IL-38	Adipogen	Cat# AG-40B-0101-C010

(*Continued on next page*)

Continued

REAGENT or RESOURCE	SOURCE	IDENTIFIER
rmIL-1Ra	Bio-Techne	Cat# -RM-O1oicF
rmIL-36Ra	Bio-Techne	Cat# 2714-ML-025
IL1RAPL1 Protein, Mouse, Recombinant (Fc Tag)	Sino Biological	Cat#: 50900-M02H
IL1RAPL1 Protein, Human, Recombinant (Fc Tag)	Sino Biological	Cat#: 10177-H02H
rhIL-38 (1-152aa)	Fraunhofer Institute IME	N/A
rhIL-38 (7-152aa)	Fraunhofer Institute IME	N/A
rmIL-38	Fraunhofer Institute IME	N/A
Critical Commercial Assays		
RNAscope® Fluorescent Multiplex Detection Reagent Kit v2	Advanced Cell Diagnostics	Cat# 320850
OpalTM 7-Color Fluorescent IHC Kit	Perkin-Elmer	Cat# NEL797001KT
Fixation/Permeabilization Solution Kit	BD Biosciences	Cat# 554714
Epidermis dissociation kit	Miltenyi Biotec	Cat# 130-095-928
Human IL-17A Flex Set	BD Biosciences	Cat# 560383
Mouse IL-17A Flex Set	BD Biosciences	Cat# 560283
Mouse IL-1β Flex Set	BD Biosciences	Cat# 560232
Mouse IL-6 Flex Set	BD Biosciences	Cat# 558301
Mouse IL-23 Flex Set	BD Biosciences	Cat# 562575
Mouse IFN-γ Flex Set	BD Biosciences	Cat# 558296
Experimental Models: Organisms/Strains		
IL-38+/+ C57BL/6	Mutant Mouse Regional Resource Center	Cat# 032391-UCD; RRID: MMRRC_032391-UCD
IL-38−/− C57BL/6	Mutant Mouse Regional Resource Center	Cat# 032391-UCD; RRID: MMRRC_032391-UCD
IL1RAPL1+/+ C57BL/6	Institut Cochin, INSERM U1016	RRID:MGI:4414659
IL1RAPL1−/− C57BL/6	Institut Cochin, INSERM U1016	RRID:MGI:4414659
Heat-killed Candida albicans	InvivoGen	Cat# tlrl-hkca
Oligonucleotides		
Probe to Mm-IL1F10	Advanced Cell Diagnostics	Cat# 524771
Mm_Il1f10_1_SG QuantiTect Primer Assay	QIAGEN	Cat# QT0028422
Mm_Il1rapl1_1_SG QuantiTect Primer Assay	QIAGEN	Cat# QT00292691
Software and Algorithms		
Graph Pad Prism 8	GraphPad Software	https://www.graphpad.com/
Flowjo Vx	Tree Star	https://www.flowjo.com/
Li-Cor Odyssey Application Software V2.0	LICOR Biosciences	https://www.licor.com/bio/products/software/image_studio
FCAP software V3.0	BD Biosciences	http://www.bdbiosciences.com/us/applications/research/bead-based-immunoassays/analysis-software/fcap-array-software-v30/p/652099
InForm2.2 Software	PerkinElmer	http://www.perkinelmer.com:80/lab-products-and-services/resources/tissue-imaging-software-downloads.html

CONTACT FOR REAGENT AND RESOURCE SHARING

Further information and requests for resources and reagents should be directed to and will be fulfilled by the Lead Contact, Andreas Weigert (weigert@biochem.uni-frankfurt.de).

EXPERIMENTAL MODEL AND SUBJECT DETAILS

The IL-38 knockout mouse strain used for this research project, 129S5-*Il1f10*^{tm1Lex}/Mmucd, identification number 032391-UCD, was obtained from the Mutant Mouse Regional Resource Center, a NIH funded strain repository, and was donated to the MMRRC by Genentech, Inc. IL1RAPL1 KO mice were described before (Pavlowsky et al., 2010). All mouse experiments were approved by and followed the guidelines of the Hessian animal care and use committee (FU/1059, FU/1166, FU/1095).

Psoriasisform dermatitis model

The IMQ-induced psoriasis mouse model was performed and skin severity was assessed as previously described (van der Fits et al., 2009). Mouse back skin was shaved one day before starting the experiment. 62.5 mg commercially available cream containing 5% IMQ (Aldara; 3M Pharmaceuticals) was daily applied on the back skin of 8-10 weeks old male or female mice for 3, 5, or 6 consecutive days. Skin severity was evaluated according to PASI scoring system based on the extent of skin thickness, redness and scaling. In some experiments, 1 mg/kg body weight of human recombinant IL-38 versus control buffer, or anti-γδ TCR blocking antibody versus the isotype control were subcutaneously or i.p. injected into the shaved back skin of anesthetized WT or IL-38 KO mice for 3, 5, or 6 consecutive days followed by IMQ application. Mice were sacrificed and skin samples were harvested on day 3, day 5 or day 6 for further analyses.

In all mouse experiments, whenever possible, littermate controls were used.

METHOD DETAILS

Flow cytometry and cell sorting

For creating skin single cell suspensions, the epidermis dissociation kit (Miltenyi Biotec) was used to isolate epidermis from dermis after removing the subcutaneous fat. Epidermal single cell suspensions were then prepared according to the manufacturer's protocol. The remaining dermis was chopped into small pieces and was incubated in 300 μg/ml liberase and 50 U/ml DNase I (Merck) for 90 min to obtain single dermal cell suspensions. For intracellular flow cytometry, the whole skin was disintegrated following the dermis protocol. Single-cell suspensions were blocked with FcR blocking reagent (Miltenyi Biotec) in 0.5% PBS-BSA for 20 min, stained with fluorochrome-conjugated antibodies and analyzed on a LSR II/Fortessa flow cytometer or sorted using a FACS Aria III cell sorter (both from BD Biosciences). Data were analyzed using FlowJo Vx (TreeStar). All antibodies and secondary reagents were titrated to determine optimal concentrations. Comp-Beads (BD) were used for single-color compensation to create multicolor compensation matrices. For gating, fluorescence minus one controls were used. The instrument calibration was controlled daily using Cytometer Setup and Tracking beads (BD Biosciences). For characterization of immune cell subsets in skin the following antibodies were used: anti-CD3-PE-CF594, anti-CD4-BV711, anti-CD8-BV650, anti-CD11b-BV605, anti-CD11c-AlexaFluor700, anti-CD19-APC-H7, anti-CD326-BV711, anti-Ly6C-Per-CP-Cy5.5, anti-NK1.1 BV510 (BD Biosciences), anti-CD45-Vio-Blu, anti-MHC-II-APC (Miltenyi Biotec), anti-CD-90-PE, anti-F4/80-PE-Cy7, anti-GITR-FITC, anti-γδ TCR APC, and anti-Ly6G-APC-Cy7 (BioLegend). For intracellular cytokine analysis, single-cell suspensions were cultured with 5 μg/ml Brefeldin A solution (eBioscience) and Golgi stop (BD Biosciences) for 4h at 37°C. Cells were subsequently stained with the following cell surface markers: anti-CD3-PE-CF594, anti-CD4-BV711, anti-CD8-BV650, anti-CD11b-BV605, anti-CD19-APC-H7, anti-CD326 (EpCAM)-BV711, anti-Ly6C-Per-CP-Cy5.5, anti-NK1.1 BV510 (BD Biosciences), anti-CD45-Vio-Blu, anti-F4/80-PE-Cy7, anti-γδ TCR APC, and anti-Ly6G-APC-Cy7 (BioLegend). Cells were then fixed, permeabilized (BD Biosciences), and stained with anti-IL-17A PE and/or anti-IFN-γ FITC (BD Biosciences) antibodies. For FACS-Sorting of γδ T cells, the following antibodies were used: anti-CD3-PE-CF594, anti-CD4-BV711, anti-CD8-BV650, anti-CD11b-BV605, anti-CD19-APC-H7, anti-CD326 (EpCAM)-BV711, anti-Ly6C-Per-CP-Cy5.5, anti-NK1.1 BV510 (BD Biosciences), anti-CD45-VioBlue, anti-F4/80-PE-Cy7, anti-γδ TCR APC, and anti-Ly6G-APC-Cy7 (BioLegend). For analysis of IL1RAPL1 expression on T cells, cells were fixed and permeabilized and stained with an anti-IL1RAPL1 antibody (Proteintech) and a secondary anti-rabbit-AF-594 antibody.

RNA extraction and quantitative real-time PCR

Total RNA from skin and tumor samples was extracted using pegGOLD RNAPure (Peqlab Biotechnologie) and 1 μg mRNA was used for reverse transcription with the Maxima First Strand cDNA Synthesis kit (Thermo Fisher). Quantitative real-time PCR reactions were conducted with the iQ SYBR Green Supermix (Bio-Rad), Absolute QPCR SYBR Green Mix (ABgene), and the MyiQiCycler on a CFX96 Connect system (Bio-Rad). Relative mRNA expression was analyzed based on ΔΔCt method and normalized to either Actb or Rps27A as housekeeping genes. Quantitect primer assays (QIAGEN) were used to detect murine Il1f10 and Il1rapl1. Other murine primer sequences were:

Rps27a F: 5′-GACCCTTACGGGGAAAACCAT-3′, R: 5′-AGACAAAGTCCGGCCATCTTC-3′;
Actb F: 5′-CCCTCTGAACCCTAAGGCCA-3′, R: 5′-GGGACAACACAGCCTGGATG-3′;
Il6 F: 5′-TAGTCCTTCCTACCCCAATTTCC-3′, R: 5′-TTGGTCCTTAGCCACTCCTTC-3′;
Il17a F: 5′-CCACGTCACCCTGGACTCTC-3′, R: 5′-CTCCGCATTGACACAGCG-3′;
Il23a F: 5′-ATGCTGGATTGCAGAGCAGTA-3′, R: 5′-ACGGGGCACATTATTTTTAGTCT-3′;

Il1b F: 5′-GCAACTGTTCCTGAACTCAAC-3′. R: 5′-ATCTTTTGGGGTCCGTCAACT-3′;
Ivl F: 5′-GTCCCATCAACACACACTGC-3′, R: 5′CTCCTCATGTTTGGGAAAGC-3′;
Lor F: 5′-AGAAAAAGCAGCCCACTCC-3′, R: 5′-GAACCACCTCCATAGGAACC-3′;
Krt10 F: 5′-GCCTCCTACATGGACAAAGTC-3′, R: 5′-GCTTCTCGTACCACTCCTTGA-3′.

Western Blotting

Mouse skin samples were processed into fine powder and sonicated in SDT lysis buffer. Protein in cell lysate was loaded on polyacrylamide gels followed by transfer onto nitrocellulose membranes. Membranes were then incubated with primary antibodies against Krt10 (ab76318, Abcam) and rabbit anti-GAPDH antiserum as loading control. Bands were visualized by IRDye 800- and IRDye 680-coupled secondary Abs using the Li-Cor Odyssey imaging system (LICOR Biosciences, Bad Homburg, Germany).

Production of human recombinant IL-38 variants

The design of the IL-38 constructs and the general purification strategy was described before (Mora et al., 2016). The expression and purification protocol has been changed as follows: *E. coli* Rosetta (DE3) pLysS carrying the appropriate IL-38 expression vectors were grown in 4 l of minimal medium with glucose (KH_2PO_4 16.6 g/l; $NH_4H_2PO_4$ 4 g/l; $CaCl_2 \cdot 2H_2O$ 0.07 g/l; $FeSO_4 \cdot 7H_2O$ 0.14 g/l; $MgSO_4 \cdot 7H_2O$ 1.5 g/l; citric acid 2.1 g/l; methionine 0.2 g/l; PTM1 trace salts solution 1 ml/l; glucose 25 g/l; kanamycin 0.05 g/l; pH 6.8) at 37°C in a 5 l fermenter. At glucose exhaustion, the cultures were cooled down to 28°C and fed with 18 ml/h of 500 g/l glucose with $MgSO_4 \cdot 7H_2O$ 14.7 g/l with simultaneous induction with 0.5 mM isopropyl β-D-1-thiogalactopyranoside (IPTG). 6.5 h post induction, the bacterial pellet was collected and frozen at −80°C. After thawing, the pellet was resuspended in column buffer (50 mM phosphate pH 7.5, 800 mM NaCl, 4% glycerol) supplemented with 1 mM $MgCl_2$, 10 mM 2-mercaptoethanol, 0.1 mM phenylmethanesulfonyl fluoride (PMSF), 0.5% TRITON X-100, 1 mg/mL lysozyme and 5 μg/ml DNaseI and cells were lysed by homogenization at 1450-1550 bar. The lysate was cleared by centrifugation, supplemented with 20 mM imidazole and applied on Chelating Sepharose FF column on ÄKTA pure. Column was washed with wash buffer (column buffer, 20 mM imidazole, 1 mM 2-mercaptoethanol, 0.5% TRITON X-100) and then further washed with detergent-free wash buffer. The IL-38 fusions constructs were eluted with wash buffer containing 250 mM imidazole and desalted on HiPrep 26/10 Desalting column on ÄKTA pure. Resulting samples were cleaved over night at 4°C with 5 μM HIS_6-USP2 and re-applied on Chelating Sepharose FF column. Endotoxin was removed by High-Capacity Endotoxin Removal Resin (Pierce) according to the manufacturer's protocol. The samples were sterile filtered, aliquoted, flash-frozen and stored at −80°C. The final endotoxin content was measured by LAL Chromogenic Endotoxin Quantitation Kit (Pierce) and the lack of pyrogenicity was further confirmed by absence of TNF-α release from human macrophages stimulated with IL-38 variants.

In vitro immune cell activation assays

Single-cell suspensions from mouse spleens were generated by mechanical dissociation. Red blood cell lysis buffer was used to remove the red blood cells. Obtained cell suspensions were filtered with 70-μm cell strainers (BD Biosciences). Thereafter, total cells, FACS-sorted γδ T cells or CD4+ T cells were seeded on 1 μg/ml anti-mouse CD3e-precoated 96 well plates (BD Biosciences) and stimulated with 10 ng/ml rmIL-23 (Bio-Techne), 10 ng/ml rmIL-1β (Bio-Techne) and different concentrations of full length human IL-38, mature human IL-38, rm-IL-38 (Adipogen), rmIL-1Ra, or rmIL-36Ra (both from Bio-Techne) prepared in T cell medium (RPMI supplemented with 100 U/ml penicillin, 100 mg/ml streptomycin, 10% heat-inactivated FCS, 1% MEM non-essential amino acids, 1% sodium pyruvate, and 1% HEPES buffer solution, from PAA Laboratories). Cells were then cultured for up to 7 days.

Human PBMCs were isolated from buffy coats of anonymous healthy donors (DRK-Blutspendedienst Baden-Wuerttemberg-Hessen, Institut für Transfusionsmedizin und Immunhämatologie Frankfurt am Main, Frankfurt, Germany) using Ficoll-Hypaque gradients. $5x10^5$ cells/ml were plated in medium (RPMI supplemented with 100 U/ml penicillin, 100 mg/ml streptomycin, 10% heat-inactivated FCS) in 96 well plates, followed by the stimulation with full length or mature IL-38 for 1h at 37°C. Cells were further incubated with heat-killed *Candida albicans* (InvivoGen) at a concentration of 5×10^6 cells/ml for 6 days. Supernatants were harvested for cytokine analysis at the times indicated.

Cytometric Bead Array

To determine cytokine levels in cell culture supernatants or murine tissues (in skin and tumors as described before (Weichand et al., 2017)), human IL-17A, or murine IL-17A, IL-1β, IL-6, IL-23, and IFN-γ Cytometric Bead Array Flex Sets (BD Biosciences) were used. Samples were acquired with a LSR Fortessa flow cytometer (BD Biosciences) and data was analyzed using BD Biosciences FCAP software (V3.0).

Immunohistochemistry

In situ hybridization by RNAscope® technique was performed according to the manufacturer's instructions (Advanced Cell Diagnostics (ACD)). 4μm thick sections were deparaffinized and treated with H_2O_2 followed by antigen retrieval and protease treatment according to the RNAscope Multiplex Fluorescent v2 assay kit's instructions. For murine skin sections, probes to Mm-IL1F10 ACD #524771 and positive/negative controls (probe 3-plex (POLR2A; PPIB; UBC) ACD #320881/ 3-plex negative control probe (DapB) ACD #320871) were used. Probes were hybridized for 2 h followed by 3 amplification steps. The signal was detected with

RNAscope® Multiplex fluorescent Detection reagent kit v2 (ACD #323110) using Opal dyes (PerkinElmer). Following RNAscope, skin sections were stained using the Opal staining system according to the manufacturer's instructions (PerkinElmer) using antibodies against murine Keratin 14 (Biolegend). Nuclei were counterstained with DAPI. For analyzing epidermal architecture, the OpalTM 7-Color Fluorescent IHC Kit (Perkin-Elmer) was used according to the manufacturer's instructions. Slides were stained with primary antibodies targeting Ki67, Keratin10 (both from Abcam), Keratin14, Loricrin and Involucrin (Biolegend). The Vectra® 3 automated quantitative pathology imaging system (Perkin-Elmer) was used for image acquisition at 20x and images were analyzed using inForm2.0 Software (PerkinElmer).

Expression and purification of mouse recombinant IL38

Recombinant mouse IL-38 was expressed as an N-terminal fusion protein with hexa-histidine followed by ubiquitin (His-Ub) and concluded at the C terminus with an Avi-tag (GLNDIFEAQKIEWHE) for site-specific biotinylation. The protein was expressed in BL21 (DE3) co-transformed with pBirAcm (Avidity, L.L.C., USA) plasmid that encodes for biotin-ligase A. To ensure sufficient biotinylation, D(+)-biotin (Roth) was added to the expression medium to a final concentration of 100 μM. Expression and purification were done as before, but without cleavage of the His-Ub-tag by USP2 (Mora et al., 2016). The resulting protein fractions after elution (800 mM NaCl, 400 mM Imidazole, 50 mM Na3PO4, 1 mM β-mercaptoethanol and 4% glycerol) were dialyzed in PBS (137 nM NaCl, 2.7 nM KCl, 10 nM Na2HPO4 and 1.8 nM KH2PO4 at pH 7.4).

Receptor binding assay

Mouse or human IL1RAPL1/Fc chimera (Sino Biological Inc.) were immobilized on 384 maxisorp plates (NUNC) at a concentration of 0.1 μg/well in 25 μl PBS overnight at 4°C. After blocking with 90 μl PBT-buffer (0.5% BSA, 0.1% Tween 20 in PBS) for 1 h and 4°C, a 1:1 dilution series of recombinant mouse or human His-Ub-IL-38-Avi fusion protein (0, 0.031, 0.063, 0.125, 0.25, 0.5 and 1 μM) were added to the wells and incubated for 2 h at 4°C in PBT buffer. After IL-38 binding, wells were washed 4 times with 90 μl PT buffer (0.1% Tween 20 in PBS). Subsequently, 25 μL of High Sensitivity NeutrAvidin-HRP (Thermo Fisher Scientific, diluted 1:2000 in PBT buffer) was added to the wells. After incubation for 1 h at 4°C, the plate was washed 4 times with PT buffer and 25 μl freshly prepared Tetramethylbenzidine (TMB) substrate (BD Biosciences) was added. The reaction was stopped with 25 μL 1.0 M H3PO4. Signals were read spectrophotometrically at 450 nm (Epoch, BioTek). Plotted values were corrected for background binding of mouse His-Ub-IL-38-Avi to BSA coated wells.

Analysis of publicly available human datasets

Gene expression data from a publicly available dataset (Li et al., 2014a) were retrieved from Gene Expression Omnibus (Barrett et al., 2013), and analyzed using GraphPad Prism v8

QUANTIFICATION AND STATISTICAL ANALYSIS

Data are presented as means ± SEM. Statistical comparisons between two groups were performed using Mann Whitney test, paired or unpaired two-tailed Student's t test as indicated. One- or two-way analysis of variance (ANOVA) followed by appropriate post-tests was used for multiple comparisons. Data were pre-analyzed to determine normal distribution and equal variance with D'Agostino–Pearson omnibus normality test. Statistical survival analysis was performed using the log-rank test. Correlation was analyzed using Spearman test. Statistical analysis was performed with GraphPad Prism v8. Differences were considered significant at $p < 0.05$. No statistical test was used to predetermine sample size, and all samples were included in the analysis. Details on statistical tests used in individual experiments can be found in the Figure legends.